ISSN 1063-7729, Astronomy Reports, 2012, Vol. 56, No. 3, pp. 167–178. © Pleiades Publishing, Ltd., 2012.
Original Russian Text © G.S. Bisnovatyi-Kogan, Yu.M. Krivosheev, 2012, published in Astronomicheskii Zhurnal, 2012, Vol. 89, No. 3, pp. 195–207.

A Study of Jet Heating Mechanisms with Application to the Microquasar SS 433

G. S. Bisnovatyi-Kogan[1,2] and Yu. M. Krivosheev[3*]

[1] *Space Research Institute, Russian Academy of Sciences, 84/32 Profsoyuznaya Str., Moscow 117997, Russia*

[2] *Moscow Engineering Physics Institute, National Nucear Research University, Moscow, Russia*

[3] *Space Research Institute, Russian Academy of Sciences, Profsoyuznaya ul. 84/32, Moscow, 117997 Russia*

Received August 10, 2011; in final form, August 17, 2011

Abstract—We consider various physical processes that affect the thermal balance of an X-ray jet. We focus on the rapid cooling of dense jets via bremsstrahlung, and all processes are considered from the viewpoint of their contributions to the jet thermal balance. Jet heating by Compton scattering of hard X-ray photons from the hot corona, the effect of shocks in the jet on heating of the jet, and the transformation of jet kinetic energy into heat via Coulomb collisions between protons of the jet and corona are considered. Numerical values have been obtained for the Galactic microquasar SS 433 based on previous results for modeling the X-ray spectrum of this source. Collisions of the jet particles with the ambient gas turns out to be the most important jet heating mechanism for this source.

DOI: 10.1134/S106377291203002X

1. INTRODUCTION

Jets are quite frequent in the Universe, and can have various sizes and shapes. Although their existence has been known for decades, many questions remain open, first and foremost, related to the formation, collimation, and radiation of jets. In the present paper, we consider the last of these questions, which reduces to an investigation of energy balance in the jet. We consider the X-ray jet, i.e., the region close to its base where the temperature reaches tens of keV and the matter is completely ionized. Under these conditions, the main energy-loss mechanisms are bremsstrahlung and cooling due to adiabatic expansion. The temperature profile in the jet can vary substantially, depending on the ratio radiative to expansion losses. In the source SS 433, we are dealing with a dense jet surrounded by a more rarefied corona, radiating in the hard X-ray range. As was shown in [1], the best agreement between the results of simulations and INTEGRAL observations is obtained if the ratio of the densities of the jet and corona is about 200 and only adiabatic cooling is taken into account. However, radiative cooling is appreciably higher than cooling due to expansion near the jet base. If there is no heating, this should lead to rapid cooling along the jet, moving the boundary of the X-ray ray jet down to its base, in contradiction with observations. Therefore, mechanisms supplying energy to the jet must be present, compensating for the radiative losses.

We consider here three mechanisms for jet heating.

(1) Compton scattering of hard X-ray photons of the corona on jet electrons.

(2) Heating due to shock wave energy dissipation, shocks are generated at the jet base and travel along the jet.

(3) The transformation of the jet kinetic energy into heat due to Coulomb collisions between protons of the jet and corona.

Calculations indicate that the third mechanism is important for the thermal balance of the jet in the Galactic microquasar SS 433.

2. JET THERMAL-BALANCE EQUATION

Let us write the balance equation for the internal energy of a jet, assuming that its matter is an ideal, monoatomic, non-relativistic gas. This approximation is justified in the X-ray jet, where the temperatures are high enough to bring about full ionization of the plasma, and the radiation energy is negligible due to the low optical depth across the jet:

$$\frac{d\varepsilon}{dt} = q - p\frac{dV}{dt}. \qquad (1)$$

*E-mail: krivosheev@iki.rssi.ru

Here, ε is the internal energy per unit mass of the gas, q the energy inflow or outflow per unit mass, p the pressure, and $V = 1/\rho$ the gas specific volume. If we assume that the gas flow is stationary, and the gas is moving radially with the velocity $v_{\rm jet} = 0.27c$ at each point of the jet, we have $d/dt = v_{\rm jet} d/dr$. Equation (1) then takes the form

$$v_{\rm jet}\frac{d\varepsilon}{dr} = \frac{p}{\rho^2}v_{\rm jet}\frac{d\rho}{dr} + q. \qquad (2)$$

Taking into account the relationship between the internal energy of an ideal gas with adiabatic index $\gamma = 5/3$, $\varepsilon = 3p/2\rho$, and the pressure–temperature relation, $p = nkT$ (n is the gas particle number density and k is Boltzmann's constant), and neglecting the contribution of electrons to the density $\rho = m_p n$, we bring (1) into the form

$$\frac{3}{2}\frac{v_{\rm jet}k}{m_p}\frac{dT}{dr} = \frac{v_{\rm jet}}{m_p}kT\frac{1}{\rho}\frac{d\rho}{dr} + q. \qquad (3)$$

This equation determines the dependence of the jet temperature on the radial coordinate, and, for the very narrow jet in SS 433, it essentially determines the temperature distribution along the jet.

2.1. Density Profile

Let us consider a conical jet (that is, with a constant opening angle) and assume that all particles in the jet move radially with the velocity $v_{\rm jet} = 0.27c$. Let the apex of the jet cone be at the coordinate origin. Then, if the mass flux in the jet is constant, at an arbitrary distance r along the jet axis, the amount of mass passing through the jet cross section per second is

$$\dot{M}_{\rm jet} = m_p n_{\rm jet}(r) v_{\rm jet}\pi r^2 \tan^2(\theta_{\rm jet}/2), \qquad (4)$$

which determines the radial dependence of the proton density in the hydrogen plasma, $n_{\rm jet}$:

$$n_{\rm jet}(r) = \frac{\dot{M}_{\rm jet}}{m_p v_{\rm jet}\pi r^2 \tan^2(\theta_{\rm jet}/2)}. \qquad (5)$$

The jet does not begin at the origin, but at some distance from it, r_0, where the particle density is $n_{0,\rm jet} = \dot{M}_{\rm jet}/m_p v_{\rm jet}\pi r_0^2 \tan^2(\theta_{\rm jet}/2)$. The jet mass flux and opening angle were taken to be [1] $\dot{M}_{\rm jet} = 4\times 10^{19}$ g/s and $\theta_{\rm jet} = 1.2^\circ$. We then obtain the radial dependence of the number density

$$n_{\rm jet} = n_{0,\rm jet}\left(\frac{r_0}{r}\right)^2. \qquad (6)$$

The value of $n_{0,\rm jet}$ is determined by the jet opening angle and the mass flux $\dot{M}_{\rm jet}$. As was shown in [1], the best fit of the observed X-ray spectrum of SS 433 is obtained for $n_{0,\rm jet} = 0.86\times 10^{15}$ cm^{-3}. We will use this value in our further calculations. We also have

$$\frac{1}{\rho}\frac{d\rho}{dr} = \frac{1}{n_{\rm jet}}\frac{dn_{\rm jet}}{dr} = -\frac{2}{r}. \qquad (7)$$

2.2. Bremsstrahlung Losses

Assuming that the jet material is in local thermal equilibrium, we can use Kirchhoff's law relating the absorption coefficient at frequency ν, α_ν [cm^2/g], with the emission coefficient $q^{ff}_{\nu,\theta}$ [erg g^{-1} s^{-1} sr^{-1} Hz^{-1}] in the form

$$q^{ff}_{\nu,\theta} = \alpha^{ff}_\nu B_\nu, \qquad (8)$$

where

$$B_\nu = \frac{2h}{c^2}\nu^3\frac{1}{\exp(h\nu/kT) - 1} \qquad (9)$$

is the Planck function for the equilibrium radiation intensity (see, e.g., [2]). Using the well known absorption coefficient for bremsstrahlung α^{ff}_ν, taking into account induced processes, and setting the Gaunt factor equal to unity,

$$\alpha^{ff}_\nu = \frac{4}{3}\sqrt{\frac{2\pi}{3}}\frac{e^6}{hm_p m_e\sqrt{m_e c^2}} \times \frac{n_e}{\nu^3\sqrt{kT}}\left[1 - \exp\left(-\frac{h\nu}{kT}\right)\right], \qquad (10)$$

we obtain an expression for the energy $q^{ff}_{\nu,\theta}$ emitted via bremsstrahlung from a unit mass into unit solid angle per unit time in a unit frequency band:

$$q^{ff}_{\nu,\theta} = \frac{8}{3}\sqrt{\frac{2\pi}{3}}\frac{e^6}{m_p(m_e c^2)^{3/2}}\frac{n_e}{\sqrt{kT}} \times \exp\left(-\frac{h\nu}{kT}\right). \qquad (11)$$

For simplicity, we assume that the jet plasma consists of hydrogen, so that $n_e = n_{\rm jet}$ and $\rho = m_p n_{\rm jet}$. Integrating over frequency and solid angle, we obtain an expression for the isotropic radiative losses q^{ff} per unit mass of jet material:

$$q^{ff} = \int q^{ff}_{\nu,\theta} d\nu d\theta = 16\left(\frac{2\pi}{3}\right)^{3/2} \times \frac{e^6}{hm_p m_e c^2} n_{\rm jet}\sqrt{\frac{kT}{m_e c^2}}. \qquad (12)$$

Substituting the values of the physical constants, we have

$$q^{ff} = 0.852\times 10^{-3} n_{\rm jet}\sqrt{T} \equiv D n_{\rm jet}\sqrt{T}\ {\rm erg/g\,s}. \qquad (13)$$

2.3. Solution of the Energy-Balance Equation

Using (6), (7), and (13) in (3), with $q = -q^{ff}$, we obtain the energy-balance equation

$$\frac{dT}{dr} = -\frac{4T}{3r} - \frac{2m_p}{3kv_{\rm jet}}q^{ff}. \qquad (14)$$

The temperature at the jet base $T(r_0)$ is assumed to be known,

$$T(r_0) = T_0. \qquad (15)$$

To find the relative contribution of each term on the right-hand side to cooling of the jet, we consider the ratio of the bremsstrahlung and adiabatic energy losses: $q^{\rm ad} = -2v_{\rm jet}kT/m_p r$:

$$\frac{q^{ff}}{q^{\rm ad}} = 8\left(\frac{2\pi}{3}\right)^{3/2} \qquad (16)$$
$$\times \frac{e^6}{(m_e c^2)^2 h}\frac{n_{0,\rm jet}r_0^2}{rv_{\rm jet}}\sqrt{\frac{m_e c^2}{kT}} \sim \frac{n_{\rm jet}r}{\sqrt{T}}.$$

Let us calculate this ratio at the jet base, $r = r_0 = 10^{11}$ cm, using the values $n_{0,\rm jet} = 0.86 \times 10^{15}$ cm^{-3} and $T_0 = 2.2 \times 10^8$ K obtained in [1]:

$$\frac{q^{ff}}{q^{\rm ad}} \approx 3.8. \qquad (17)$$

It is clear that bremsstrahlung losses substantially exceed adiabatic losses at the jet base.

Let us consider the solution of the equation for the jet-temperature profile (14) and compare it with the solution obtained if bremsstrahlung losses are ignored. Introducing the new variables $t = T/T_0$ and $x = r/r_0$, (14) takes the form

$$\frac{dt}{dx} = -\frac{2}{3}\left(2\frac{t}{x} + D\frac{\sqrt{t}}{x^2}\right), \quad t(1) = 1, \qquad (18)$$

where α is given by

$$D = 16\left(\frac{2\pi}{3}\right)^{3/2}\frac{e^6}{h(m_e c^2)^{3/2}}\frac{n_{0,\rm jet}r_0}{v_{\rm jet}\sqrt{kT_0}}. \qquad (19)$$

Equation (18) was studied by Koval' and Shakura [3], who found its solution in the form

$$\frac{T}{T_0} = \left(\frac{r_0}{r}\right)^{4/3}\left\{1 - D\left[1 - \left(\frac{r_0}{r}\right)^{1/3}\right]\right\}^2. \qquad (20)$$

The factor before the curly brackets corresponds to the temperature change due to expansion, while the factor inside the curly brackets is determined by the bremsstrahlung losses. The coefficient D characterizes the ratio of bremsstrahlung to expansion losses. The case $D \ll 1$ corresponds to small bremsstrahlung losses at the jet base, in which case the temperature distribution differs little from the case of adiabatic expansion. However, in our case, the opposite case is realized: $D = 2q^{ff}/q^{\rm ad}(r_0) \approx 7.6$. Therefore, the temperature distribution differs strongly from that obtained for adiabatic expansion. The jet will be cooled much more rapidly, and the boundary of the X-ray jet will move closer to the base, so that, according to (20), the temperature formally becomes zero as close as $r = 1.6r_0 = 1.6 \times 10^{11}$ cm.

The dotted line in Fig. 1 was obtained with only bremsstrahlung taken into account. In our further calculations, we will use a more realistic tempera-

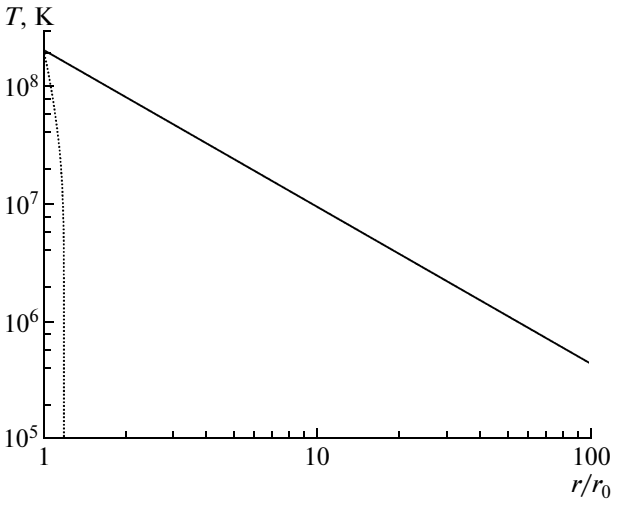

Fig. 1. Jet temperature profiles taking only adiabatic losses (solid) and also into account bremsstrahlung losses (dotted).

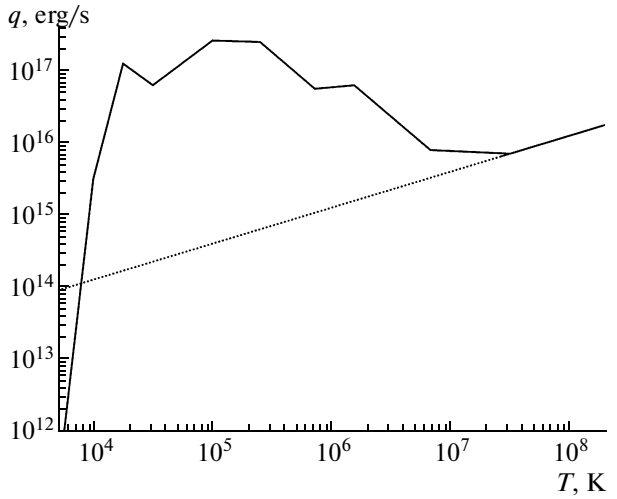

Fig. 2. Plots of the radiative cooling rate taking into account only bremsstrahlung (dotted) and with bound-free and bound-bound transitions included (solid).

ture dependence for the plasma radiative cooling rate, based on an approximation of the numerical computations [4–7] using an analytic expression taking into account free–bound and bound–bound transitions [8].

Figure 2 presents this realistic cooling rate, $q_{\rm br}(T)$, and the cooling rate due to bremsstrahlung only, $q^{ff}(T)$. The radiative cooling rate including the bound states increases strongly at temperatures $T < 10^7$ K, and we expect that the jet should rapidly cool after its temperature falls to this value.

The temperature distribution obtained taking into account radiative cooling does not agree with the observations, which indicate that the boundary of the X-ray jet should be located at a distance of $r_1 \approx 10^{13}$ cm $= 100 r_0$. Obviously, some heating mechanisms must be operating, and supplying the jet with energy that compensates for the radiative losses.

3. THE INFLUENCE OF COMPTON SCATTERING ON THE JET THERMAL BALANCE

The jet material is subjected to radiation coming from the inner parts of the accretion disk, as well as bremsstrahlung from the hot corona. We can thus consider the ejected material to pass through and interact with a photon gas. Since we are interested in the X-ray jet, where the temperatures are of the order of 1 keV, the main form of interaction between the jet material and the radiation is scattering on free electrons (the Compton effect). Let us consider the influence of Compton scattering on the jet thermal balance.

3.1. Photon Energy Density

The energy density of photons with frequency ν is equal to a sum of the energy densities of photons emitted by the accretion disk and the corona:

$$\varepsilon_\nu^{\rm tot} = \varepsilon_\nu^{\rm cor} + \varepsilon_\nu^{\rm disk}. \qquad (21)$$

The accretion disk luminosity $L_{\rm disk}$ is assumed to be $0.1 L_{cr}$ [1]. The spectral energy density of the disk photons a distance r along the jet axis is equal to

$$\varepsilon_\nu^{\rm disk} = \frac{L_{{\rm disk},\nu}}{c\Omega_{\rm disk} r^2}. \qquad (22)$$

Here, $\Omega_{\rm disk}$ is the solid angle into which the disk emits, $\Omega_{\rm disk} = 2\pi(1 - \sin\theta_{\rm disk}/2)$. The disk emits an equilibrium photon flux. Due to a low optical depth of the jet, the energy density of the emitted photons does not depend on the presence or absence of the jet, and is everywhere given approximately by (22). The integrated energy density of the disk photons is

$$\varepsilon^{\rm disk} = \frac{L_{\rm disk}}{c\Omega_{\rm disk} r^2}. \qquad (23)$$

We assume that the (hydrogen) corona is in a state of local thermal equilibrium, and the proton density in the corona is $n_{\rm cor} = n_e$, so that a unit volume of coronal matter emits into unit solid angle per unit frequency per unit time an energy $\rho q_{\nu,\theta} = k_\nu B_\nu n_{\rm cor}^2$ (erg s^{-1} cm^{-3} sr^{-1} Hz^{-1}), and the total radiation is obtained by multiplying this by 4π. Since the photons travel at the speed of light and are collected at each point of the corona or jet from a volume with the characteristic size of the corona $r_{\rm cor}$, the density of photons with frequency ν emitted by the corona is approximately the same in the corona and the jet:

$$\varepsilon_\nu^{\rm cor} = 4\pi k_\nu B_\nu \bar{n}_{\rm cor}^2 \frac{r_{\rm cor}}{c}, \qquad (24)$$

$$k_\nu = \frac{\alpha_\nu m_p}{n_{\rm cor}}.$$

Here, k_ν does not depend on the matter density. For a radial dependence of the corona density similar to the corresponding dependence (6) in the jet, the mean square particle density in the corona is equal to

$$\bar{n}_{\rm cor}^2 = 3 n_{0,\,\rm cor}^2 \left(\frac{r_0}{r_{\rm cor}}\right)^3.$$

The spectral energy density of the Planck equilibrium radiation $\varepsilon_\nu^{\rm pl}$ is related to the intensity as $\varepsilon_\nu^{\rm pl} = 4\pi B_\nu/c$, and, using the definition of the corona spectral optical depth, $\tau_\nu^{\rm cor} = \alpha_\nu \rho r_{\rm cor} \ll 1$, we obtain for the spectral energy density of the photons emitted by the corona

$$\varepsilon_\nu^{\rm cor} = 4\pi k_\nu B_\nu \bar{n}_{\rm cor}^2 \frac{r_{\rm cor}}{c} = \tau_\nu^{\rm cor} \varepsilon_\nu^{\rm pl}. \qquad (25)$$

This corresponds to the plasma's own radiation density comprising a fraction $\tau_\nu^{\rm cor}$ of the equilibrium density at low optical depth. With (9) and (10), we finally obtain for the bremsstrahlung from (25)

$$\varepsilon_\nu^{\rm cor} = 48 \left(\frac{2\pi}{3}\right)^{3/2} \frac{e^6}{c(m_e c^2)^{3/2}\sqrt{kT_{\rm cor}}} \qquad (26)$$

$$\times \exp\left(-\frac{h\nu}{kT_{\rm cor}}\right) n_{0,\,\rm cor}^2 r_{\rm cor} \left(\frac{r_0}{r_{\rm cor}}\right)^3$$

$$= 3 q_{{\rm cor},\nu}^{ff}(r_0) m_p n_{0,\,\rm cor} \frac{r_{\rm cor}}{c} \left(\frac{r_0}{r_{\rm cor}}\right)^3.$$

The total energy density of the coronal photons is found by integrating (26) over the frequency:

$$\varepsilon^{\rm cor} = 3 q_{0,\,\rm cor}^{ff} m_p n_{0,\,\rm cor} \frac{r_{\rm cor}}{c} \left(\frac{r_0}{r_{\rm cor}}\right)^3. \qquad (27)$$

$q^{ff}_{\rm cor}$ is determined similarly to (12) with $n_{\rm jet}$ replaced by $n_{\rm cor}$.

3.2. Contribution of Comptonization to the Jet Thermal Balance

If a photon of frequency ν is scattered on a free electron moving with velocity βc (with the Lorentz factor $\gamma = 1/\sqrt{1-\beta^2}$), its frequency changes as follows [9]:

$$\nu' = \nu\frac{1-\mu\beta}{1-\mu'\beta + h\nu/\gamma m_e c^2(1-\cos\phi)}, \qquad (28)$$

where μ and μ' are the cosines of the angles between the directions of the photon and electron in the laboratory frame before and after scattering, respectively, and ϕ is the angle between the initial and final directions of the photon (the scattering angle) in the laboratory frame. Since the photon energies are of the order of 10 keV in our case, with $h\nu/m_e c^2 \ll 1$ and $\beta_{\rm jet} = 0.27 < 1$, we can expand (28) to first order in each small parameter, which yields the relative photon frequency change

$$\frac{\Delta\nu}{\nu} = \frac{\nu'-\nu}{\nu} \approx \beta\left(\mu'-\mu\right) - \frac{h\nu}{m_e c^2}\left(1-\cos\phi\right). \qquad (29)$$

Let us neglect the effect of the electron recoil (the term with $h\nu/m_e c^2$) due to its smallness compared to the frequency change due to the Doppler effect (the term with β). The energy of photons from the accretion disk is small compared to the jet temperature near its base, and the energy of photons from the corona does not exceed this temperature; therefore, with an isotropic momentum distribution for the electrons, Compton cooling of the electrons should occur. Near the jet base, the thermal components of the electron velocities are comparable to the velocity of the ordered motion ($\beta_{\rm th} \sim 0.3c$), therefore their directional distribution is not very different from the isotropic case, and Compton cooling of the electrons occurs. As the jet cools, the thermal component of the velocity becomes small compared to the velocity of the ordered motion. Then, Comptonization begins to heat the jet, since the scattered photons create a chaotic component of the electron momentum, thereby increasing their temperature. To estimate the photon frequency changes in both cases, we set the difference of the cosines in the first term equal to unity:

$$\frac{\Delta\nu}{\nu} \approx \beta. \qquad (30)$$

The frequency change will be positive for cooling and negative for heating.

Let us estimate the Compton heating. The amount of energy given by photons to a unit mass of the jet due to Comptonization is given by the expression

$$q_C \approx \frac{\sigma_T c}{m_p}\int d\nu h\Delta\nu\frac{\varepsilon_\nu}{h\nu}, \qquad (31)$$

where $\sigma_T = 6.65\times10^{-25}$ cm^2 is the Thomson scattering cross section. Substituting Eq. (30) for the frequency change into (31) and integrating yields

$$q_C = \frac{\sigma_T c}{m_p}\beta\varepsilon^{\rm tot} = \frac{\sigma_T c}{m_p}\beta(\varepsilon^{\rm cor}+\varepsilon^{\rm disk}). \qquad (32)$$

Let us find the ratio of the Compton heating rate and the cooling rate due to bremsstrahlung. Expressing the energy density of the coronal photons in terms of the emissivity per unit mass using (27), we obtain

$$q_C = 3\sigma_T\beta n_{0,\,\rm cor} r_{\rm cor} q^{ff}_{0,\,\rm cor}\left(\frac{r_0}{r_{\rm cor}}\right)^3 \times\left[1+\frac{\varepsilon^{\rm disk}}{\varepsilon^{\rm cor}}\right]. \qquad (33)$$

Using the relation

$$q^{ff}_{0,\,\rm cor} = q^{ff}_{0,\rm jet}\frac{n_{0,\,\rm cor}}{n_{0,\rm jet}}\sqrt{\frac{T_{0,\,\rm cor}}{T_{0,\rm jet}}}, \qquad (34)$$

we obtain an estimate for the ratio of the Compton contribution to the jet thermal balance to the cooling due to bremsstrahlung:

$$\frac{q_C}{q^{ff}_{0,\rm jet}} = 3\sigma_T r_{\rm cor}\frac{n^2_{0,\,\rm cor}}{n_{0,\rm jet}} \times\sqrt{\frac{T_{0,\,\rm cor}}{T_{0,\rm jet}}}\beta\left(\frac{r_0}{r_{\rm cor}}\right)^3\left(1+\frac{\varepsilon^{\rm disk}}{\varepsilon^{\rm cor}}\right) \ll 1, \qquad (35)$$

using the fact that $n_{0,\,\rm cor}/n_{0,\rm jet} = 0.005$, $r_0/r_{\rm cor} = 0.01$, and both $\varepsilon^{\rm disk}/\varepsilon^{\rm cor}$ and $3\sigma_T r_{\rm cor} n_{0,\,\rm cor}\times\beta\sqrt{\frac{T_{0,\,\rm cor}}{T_{0,\rm jet}}}$ are of the order of unity.

Thus the contribution of Comptonization is small compared to radiative cooling. The contribution of photons emitted by other processes exceeds the energy of the bremsstrahlung photons by no more than a factor of 10^3 (Fig. 2), which does not change this conclusion. Therefore, we will not include the change in the jet energy balance due to Comptonization in our further analysis.

4. JET HEATING BY THE DISSIPATION OF SHOCK ENERGY

Let us consider heating of the jet by shocks created near its base by turbulent or convective motions. We suppose that a shock with Mach number M_0 originates at the jet base, $r = r_0$. The relationships between thermodynamic quantities behind and in front of the shock front can be found from the conservation laws. For an ideal gas with adiabatic index γ, the jumps in the pressure p, specific volume $V = 1/\rho$, and temperature T at a shock front are given by the Hugoniot adiabat [10]:

$$\frac{p_1}{p_0} = \frac{2\gamma M^2}{\gamma+1} - \frac{\gamma-1}{\gamma+1}, \tag{36}$$

$$\frac{V_1}{V_0} = 1 - 2\frac{M^2-1}{M^2(\gamma+1)}, \tag{37}$$

$$\frac{T_1}{T_0} = \frac{1}{(\gamma+1)M^2} \tag{38}$$

$$\times \left[2\gamma M^2 - (\gamma-1)\right]\left[(\gamma-1)M^2+2\right].$$

Here, the subscripts 0 and 1 refer to values in front of and behind the shock front, respectively. After the passage of the shock front, the entropy per unit mass increases by the amount [10]

$$\Delta S = c_V \ln\left[\frac{p_1}{p_0}\left(\frac{V_1}{V_0}\right)^{\gamma}\right], \tag{39}$$

where $c_V = k/(\gamma-1)m_p$ is the heat capacity at constant volume per unit mass of gas. Substituting the pressure (36) and the specific volume jump (37) at the front into (39), we obtain for the entropy jump per unit mass

$$\Delta S = \frac{k}{(\gamma-1)m_p}\left[\ln\left(\frac{2\gamma M^2}{\gamma+1} - \frac{\gamma-1}{\gamma+1}\right)\right. \tag{40}$$

$$\left. + \gamma \ln\left(\frac{\gamma-1}{\gamma+1} + \frac{2}{M^2(\gamma+1)}\right)\right].$$

This expression has been obtained for a single shock propagating along the jet. However, we are interested in a stationary pattern of shocks travelling along the jet with a time interval Δt between them. Such a stationary state will be characterized by the mean temperature T for this time interval. The mean heating per unit mass of jet material per unit time due to the shocks will then be approximately equal to

$$q_{sw} \approx \frac{T\Delta S}{\Delta t} \tag{41}$$

$$= \frac{kT}{(\gamma-1)m_p\Delta t}\left[\ln\left(\frac{2\gamma M^2}{\gamma+1} - \frac{\gamma-1}{\gamma+1}\right)\right.$$

$$\left. + \gamma \ln\left(\frac{\gamma-1}{\gamma+1} + \frac{2}{M^2(\gamma+1)}\right)\right].$$

This expression determines the heating in the balance equation for the internal energy. The quantity Δt can be approximated from observations. The object SS 433 shows X-ray variability on time scales down to a few seconds [11]; therefore, to obtain an upper estimate for the shock heating, we should take $\Delta t = 1$ s. Equation (41) also contains the Mach number, which decreases as the shock front moves along the jet, due to radiative losses. To close the set of equations, we obtain an equation determining the changes in the shock energy flux as it travels along the jet.

In a coordinate system moving with the average jet motion, the shock-front velocity is $D = Mc_s$, where c_s is the local sound speed in the unperturbed gas. The kinetic energy density in such a wave is given by [12]

$$E = \frac{\rho_0}{2}v^2, \tag{42}$$

where ρ_0 is the unperturbed gas density and v is the difference of the velocities of the perturbed and unperturbed gas. It follows from the conservation laws at the shock front that [10]

$$v = \sqrt{(p_1 - p_0)(V_0 - V_1)}. \tag{43}$$

Using the relations (36), (37), and $c_s = \sqrt{\gamma p_0 V_0}$, we obtain

$$v = \frac{2(M^2-1)}{M(\gamma+1)}c_s. \tag{44}$$

The shock energy flux density, equal to the energy crossing a unit area per unit time, is equal to

$$F = ED = \frac{2(M^2-1)^2}{(\gamma+1)^2 M}\rho_0 c_s^3. \tag{45}$$

The shock energy is dissipated at the front, and is transformed into the internal energy of the gas behind the front. The rate of decrease of the energy flux density is determined by the mean heating rate per unit volume of matter behind the front:

$$\frac{dF}{dr} = -\rho_1 q_{sw}. \tag{46}$$

Using (45), the derivative dF/dr takes the form

$$\frac{dF}{dr} = \frac{2(M^2-1)}{(\gamma+1)^2}\rho_0 c_s^3\left[\left(3 + \frac{1}{M^2}\right)\frac{dM}{dr}\right. \tag{47}$$

$$\left. + \frac{M^2-1}{M}\left(\frac{1}{\rho_0}\frac{d\rho_0}{dr} + \frac{3}{2T}\frac{dT}{dr}\right)\right].$$

Let us write an equation for the decrease in the Mach number of the shock as it moves along the jet,

using (36), (46), and (47):

$$\frac{2(M^2-1)}{(\gamma+1)^2}\rho_0 c_s^3\left[\left(3+\frac{1}{M^2}\right)\frac{dM}{dr}\right. \quad (48)$$
$$\left.+\frac{1}{M}(M^2-1)\left(\frac{1}{\rho_0}\frac{d\rho_0}{dr}+\frac{3}{2T}\frac{dT}{dr}\right)\right]$$
$$=-\rho_0\frac{(\gamma+1)M^2}{2+(\gamma-1)M^2}q_{sw}.$$

An equation for the mean jet temperature resulting from the passage of the shock fronts created at the jet base follows from the thermal energy balance, whose basis is the first law of thermodynamics, and can be written

$$\frac{1}{\gamma-1}\frac{dT}{dr}=\frac{T}{\rho_0}\frac{d\rho_0}{dr}+\frac{m_p}{k}\left(\frac{q_{sw}}{Mc_s}-\frac{q_{\rm br}}{v_{\rm jet}}\right). \quad (49)$$

Here, we have used for the term determining heating by the passage of the shocks the relationship between the temporal and radial derivatives for a quasi-stationary distribution of the parameters in the coordinate frame moving with the jet mean velocity:

$$dt=\frac{dr}{D}=\frac{dr}{Mc_s}.$$

For a given density distribution $\rho_0(r)$, (48) and (49) represent a closed system of equations for the radial dependence of the temperature and the Mach number in a quasi-stationary jet heated by shocks emerging near its base. The boundary conditions at the jet base are specified in the form

$$\begin{cases}T(r_0)=T_0,\\ M(r_0)=M_0.\end{cases} \quad (50)$$

The unperturbed (mean) density profile in the jet is specified by $\rho_0(r)=m_p n_{0,\rm jet}\left(\frac{r_0}{r}\right)^2$, so $\frac{1}{\rho_0}\frac{d\rho_0}{dr}=-\frac{2}{r}$. In its rest frame, the jet has the equation of state of a non-relativistic ideal gas with $\gamma=5/3$. Thus, there remain two unknown functions in the system: $T(r)$ and $M(r)$.

We obtained the numerical solution using the Runge–Kutta method with adaptive stepsize. Figure 3 presents solutions to the system (48), (49) with the boundary conditions (50) for various shock Mach numbers.

It is clear from Fig. 3 that sufficiently strong shocks can not only compensate the bremsstrahlung losses, but also additionally heat the jet. The shock energy dissipates in a narrow region near the jet base, $\Delta r\sim(1.2{-}1.5)r_0$, beyond which the shock heating is insignificant, and the jet cools rapidly without additional heating.

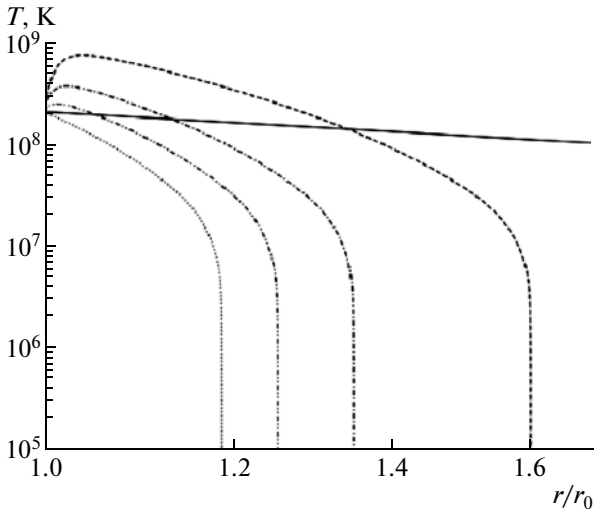

Fig. 3. Change in the jet temperature profile due to heating by shocks. The various curves correspond to shocks with Mach number $M=5$ (dashed), $M=3$ (dot–dash), and $M=2$ (double-dot–dash). The dotted curve show the temperature profile without shock heating, and the solid curve corresponds to adiabatic expansion. The value of r_0 is 10^{11} cm.

We have assumed that the shocks form near the jet base, but, in general, this is not necessary. As is known from hydrodynamics, in any wave with a convex profile, sooner or later, will develop a discontinuity in its profile due to the different sound speeds in its different parts, and the wave is converted (transformed) into a shock if this is not prevented by dissipative processes [10]. This transformation occurs even more rapidly if the wave is traveling along a decreasing density profile, as is the case in a jet. Let us suppose that the energy dissipation in a propagating compression wave can be neglected until the wave is converted to a shock. The distance at which the wave becomes a shock depends on the characteristic size of the perturbed region (the wavelength) λ, the initial magnitude of the wave, characterized by the ratio $c_{s,m}/c_{s,0}$ of the sound speeds at maximum compression and in the unperturbed medium, and the law for the density decrease. For a longer wave, more time is required for it to be transformed into a shock, but, the larger its initial amplitude and the higher the wave velocity, the earlier this conversion will happen.

To demonstrate the effect of shock dissipation at some distance from the jet base, we considered the case of shock formation at a distance of 1.15×10^{11} cm from the jet base. Figure 4 shows the solutions to the thermal balance equations with initial temperatures corresponding to adiabatic expansion.

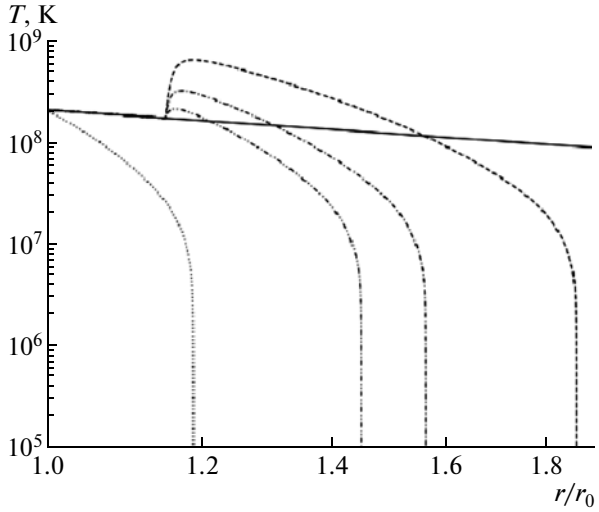

Fig. 4. Jet heating by a shock forming at a distance of 1.15×10^{11} cm from the jet base, for Mach numbers $M = 5$ (dashed), $M = 3$ (dot–dash), and $M = 2$ (double-dot–dash). The dotted curve is the gas temperature profile without shock heating, and the solid curve corresponds to adiabatic expansion.

The thickness of the shock-heated layer remains the same as in Fig. 3, and grows only if the initial Mach number grows. However, already at $M = 5$, the temperature near the shock approaches 10^9 K, in contradiction with observations; thus, growth in the Mach number cannot substantially increase the thickness of the region of heating.

The results of calculations of the thermal balance of a jet heated by shock dissipation shows that this heating is only significant when shocks can form along the entire jet, since the shocks rapidly dissipate due to radiation, and heat only narrow regions near their places of origin. Shock formation in the entire jet is possible, due both to the action of a wide spectrum of initial perturbations and interactions of the jet with the ambient medium. The latter mechanism was invoked in [13] to explain X-ray heating of the jet in the source SS 433.

5. COULOMB COLLISIONS OF PROTONS

5.1. Physics of the Process and Estimates

Consider heating of the jet due to Coulomb collisions between jet protons and protons of the ambient plasma. Thermal protons from the corona arriving at the jet serve as targets on which jet protons moving at the velocity $v_{\rm jet} = 0.27c$ are scattered. The jet protons lose some fraction of their kinetic energy in this process, giving it to the protons of the corona. The energy of the directed motion of the jet protons is converted into the energy of chaotic motions, i.e., into thermal energy. Let us estimate the maximum heating that can be obtained from this mechanism.

The number of particles obeying a Maxwellian distribution passing through a unit area per unit time is $nv_{\rm th}/4$ [14], where n is the particle density and $v_{\rm th} = \sqrt{8kT/\pi m}$ the mean velocity of the thermal motion. The jet protons can spend a maximum kinetic energy of $m_p v_{\rm jet}^2/2$ to accelerate a coronal proton to the velocity $v_{\rm jet}$. Therefore, the amount of jet kinetic energy converted to heat per unit time per unit mass of the jet is given by

$$q_{\rm coll,\,max} = v_{\rm jet}^2 \frac{v_{\rm th}}{2d_{\rm jet}} \frac{n_{\rm cor}}{n_{\rm jet}} \sim \frac{1}{r}. \qquad (51)$$

We consider here a conical jet with cross-sectional diameter $d_{\rm jet} = 2r\tan(\theta_{\rm jet}/2)$, with the radial dependence of the density in the jet and the corona having the forms $n_{\rm jet} = n_{0,\rm jet}(r_0/r)^2$ and $n_{\rm cor} = n_{0,\rm cor}(r_0/r)^2$, respectively. The amount of energy lost to bremsstrahlung per unit mass of jet per unit time is given by (13). The number densities in the corona and jet obtained in [1] are $n_{0,\rm cor} = 4.3 \times 10^{12}$ cm^{-3} and $n_{0,\rm jet} = 0.86 \times 10^{15}$ cm^{-3}. The ratio of collisional heating to bremsstrahlung will then be

$$\frac{q_{\rm coll,max}}{q_{\rm br}} = 1.56 \left(\frac{r}{r_0}\right)^{5/3}. \qquad (52)$$

This ratio grows with distance r along the jet, but, if the temperature falls below 10^7 K, the total radiative losses $q_{\rm br}$ become much stronger than the bremsstrahlung losses (Fig. 2), so that this ratio takes on its highest value at $r \approx 6.4r_0$, where it is equal to

$$\frac{q_{\rm coll,max}}{q_{\rm br}} \approx 34. \qquad (53)$$

This is an upper estimate for the ratio $q_{\rm coll}/q_{\rm br}$, since it rests on the assumption that the entire kinetic energy of jet protons is transformed into heat. In reality, the jet is fairly optically thin to protons with respect to Coulomb scattering in the transverse direction, so that the coronal protons can gain only a substantially lower fraction of the jet proton energy, which diminishes its heating accordingly.

5.2. Quantitative Treatment

For simplicity, we will neglect the thermal velocities of the coronal protons after they arrive at the jet, since they are two orders of magnitude lower than the directed velocity of the jet protons. We also neglect relativistic effects, because the jet Lorentz factor is not very much different from unity: $\gamma =$

$1/\sqrt{1-v_{\rm jet}^2/c^2} \approx 1.04$. Consider a non-relativistic proton scattered on a proton at rest. We can derive an expression for the energy gained by the proton at rest during the collision as follows.

For an elastic collision of particles of equal mass, one of which is at rest before the collision, the particle velocities after the interaction are given by [15]

$$\begin{cases} v'_{\rm mov} = v\cos(\chi/2), \\ v'_{\rm rest} = v\sin(\chi/2), \end{cases}$$

where v is the velocity of the initially moving particle in the laboratory frame, χ is the deflection angle of the scattered particle in the center-of-mass frame. For a particle in the Coulomb field with impact parameter ρ, the angle χ is equal to [15]

$$\chi = \pi - 2\arccos\frac{e^2/mv^2\rho}{\sqrt{1+(e^2/mv^2\rho)^2}},$$

where m is the mass of the scattered particles, ρ the impact parameter, and e the proton charge. In our cases, the scattered protons have $v = v_{\rm jet}$.

Let us denote $\rho_p = e^2/m_p v_{\rm jet}^2$, which is the distance of closest approach of the protons. The velocity of the proton initially at rest after the collision is

$$v'_{\rm rest} = v_{\rm jet}\frac{\rho_p/\rho}{\sqrt{1+(\rho_p/\rho)^2}}.$$

The amount of energy gained by the proton initially at rest is

$$\Delta E = \frac{m_p}{2}v'^2_{\rm rest} = \frac{m_p}{2}v_{\rm jet}^2\frac{1}{1+(\rho/\rho_p)^2}. \qquad (54)$$

To estimate the fraction of the kinetic energy of the jet proton given to the coronal proton, we can calculate a quantity similar to the optical depth with respect to Coulomb scattering in the transverse direction in the jet:

$$\tau_{\rm coll\,0} = n_{\rm jet}d_{\rm jet}\frac{2\int d\sigma\Delta E}{m_p v_{\rm jet}^2}. \qquad (55)$$

This quantity characterizes the amount of energy gained by the coronal proton as it passes through the jet in the transverse direction in units of the kinetic energy of a jet proton. The factor with the integral is equal to

$$\frac{2}{m_p v_{\rm jet}^2}\int\limits_{\rho_{\rm min}}^{\rho_{\rm max}}\Delta E d\sigma \qquad (56)$$

$$= \pi\rho_p^2\left\{\ln\left[1+\left(\frac{\rho_{\rm max}}{\rho_p}\right)^2\right] - \ln\left[1+\left(\frac{\rho_{\rm min}}{\rho_p}\right)^2\right]\right\},$$

where $d\sigma = 2\pi\rho d\rho$ is the differential cross section of the collisions, and $\rho_{\rm max}$ and $\rho_{\rm min}$ are the maximum and minimum impact parameters. We assume that the maximum impact parameter is equal to the Debye shielding radius in the jet: $\rho_{\rm max} = \lambda_D = \sqrt{kT_{\rm jet}/4\pi e^2 n_{\rm jet}}$. We take the minimum impact parameter to be equal to the classical minimum distance of approach, $\rho_{\rm min} = e^2/m_p v_{\rm jet}^2 = \rho_p$. For the jet parameters, $\rho_{\rm max} \gg \rho_{\rm min}$, and neglecting the unity in both logarithms, we obtain the Coulomb logarithm in the Landau approximation [16]:

$$\frac{1}{m_p v_{\rm jet}^2/2}\int\Delta E d\sigma = 2\pi\rho_p^2\ln\left(\frac{\lambda_D}{\rho_p}\right). \qquad (57)$$

Substituting into (55) the numerical values at $r = 6.4\times10^{11}$ cm, where we have [1] $\rho_p \approx 2.1\times10^{-15}$ cm, $n_{\rm jet} = n_{0,\rm jet}/41 \approx 2\times10^{13}$ cm^{-3}, $d_{\rm jet} = 2r\tan(\theta_{\rm jet}/2) \approx 1.3\times10^{10}$ cm, and $\ln\left(\frac{\lambda_D}{\rho_p}\right) \approx 25$, we find that $\tau_{\rm coll\,0} \approx 2\times10^{-4}$. Therefore, instead of the value obtained in (53) the ratio $q_{\rm coll}/q_{\rm br}$ is reduced to

$$\frac{q_{\rm coll}}{q_{\rm br}} \approx 6\times10^{-3}. \qquad (58)$$

The energy inflow due to Coulomb collisions can compensate about 1% of the bremsstrahlung energy losses. We assumed that the coronal protons cross the jet in the transverse direction; this provides only a lower limit for the heating. Crossing the jet at other angles, and also, even more importantly, the existence of a magnetic field, increase the time spent by the coronal protons in the jet and thereby increase the energy gained.

5.3. Influence of the Magnetic Field

The presence of a magnetic field, which necessarily exists in the ejected gas, can increase the heating due to Coulomb collisions by deflecting the trajectories of the coronal protons and increasing the time they spend in the jet, thus effectively increasing the jet's optical depth to Coulomb scattering. In order for Coulomb collisions to compensate for the radiative losses, the proton path in the jet must increase by at least two orders of magnitude [see (58)]. Let us estimate the magnetic field $B_{\rm jet}$ for which the Larmor radius of a proton would be equal to the jet radius. Let a coronal proton move in a circular path in the magnetic field with a linear velocity equal to its thermal velocity. The Larmor radius of such a proton is

$$r_L = \frac{m_p c}{eB}v_{\rm th}.$$

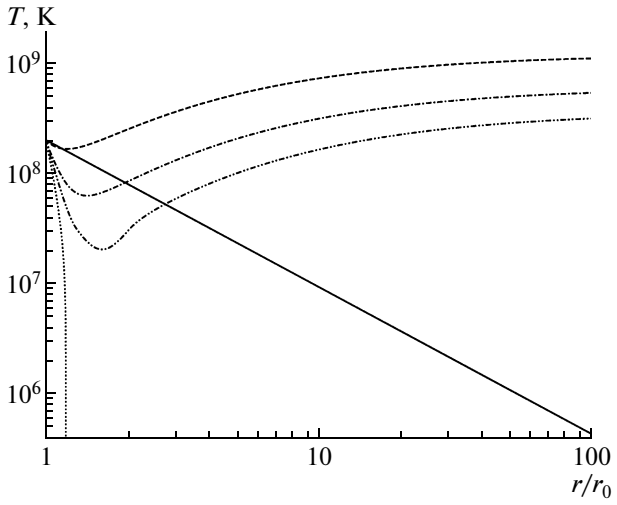

Fig. 5. Temperature profile in a jet taking into account radiative cooling and heating by Coulomb collisions with $a = 1.0$ (dashed), $a = 0.5$ (dot-dashed), and $a = 0.3$ (double-dot—dash) (see (61)). The solid curve corresponds to pure adiabatic cooling, and the dotted curve to radiative cooling only.

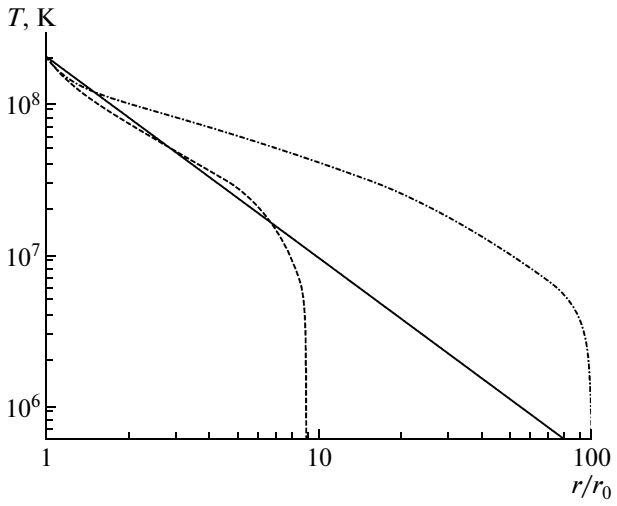

Fig. 6. Temperature profile in a jet taking into account radiative cooling and heating by Coulomb collisions with $a = (r/r_0)^{-3/2}$ (dashed) and $a = (r/r_0)^{-1.163}$ (dot-dashed) (see(61)). The solid curve corresponds to pure adiabatic cooling.

When $r_L = r_{\rm jet}$, we obtain

$$B_{\rm jet} = \frac{m_p c v_{\rm th}}{e r_{\rm jet}}. \qquad (59)$$

Since we assume that the corona is isothermal [1], the thermal velocity of the coronal protons is constant and does not depend on the distance from the jet base. Therefore, the strongest magnetic field is required near the jet base, $r_{0,\rm jet} = r_0 \tan(\theta_{\rm jet}/2) \approx 10^9$ cm. Substituting this numerical value into (59), we find that the field must be greater than

$$B_{0,\rm jet} \approx 1.3 \times 10^{-4}\ {\rm G}. \qquad (60)$$

This value of $B_{0,\rm jet}$ is so small that, in reality, the magnetic field should be greater by several orders of magnitude, i.e., $B_{\rm jet} \gg B_{0,\rm jet}$ and $\tau_{\rm coll} \gg \tau_{\rm coll\,0}$. Therefore we will assume that the coronal protons spend enough time in the jet to gain a significant amount of energy. Since the variation of the magnetic field with radius is not known, to simulate the radial dependence of the magnetic field, we introduced the function $a(r)$ characterizing the fraction of the maximum heating by Coulomb collisions that is achieved:

$$q_{\rm coll}(r) = q_{\rm coll,max}(r) a(r). \qquad (61)$$

Figure 5 presents calculated temperature profiles in the jet taking into account radiative cooling and heating by Coulomb collisions, with the function $a = {\rm const}$. Figure 5 shows that Coulomb collisions can heat the jet effectively, but the weak decrease of the collision term with radius leads to excessive jet heating at large distances. Consequently, the function $a(r)$ must decrease with distance.

Figure 6 presents the results of calculations with power-law functions $a(r)$ with various exponents. It is clear that, when the temperature $\approx 10^7$ K is reached, the jet begins to strongly cool, and this cooling is not compensated by collisions. This is due to the nature of the radiative cooling curve. At higher temperatures, collisions heat the jet efficiently. The case of the power-law exponent equal to $3/2$ approximates well the adiabatic curve for distances to $10r_0$, which can explain the X-ray observations [1], while an exponent of 1.163 provides heating that is too strong in the entire X-ray region of the jet.

5.4. Heating of the Optical Jet in SS 433

The optical jet in SS 433, which is located at $r \sim 10^{14}$–10^{15} cm $= (10^3$–$10^4) r_0$, has an approximately constant temperature, $T \sim 10^4$ K [17]. This means that there must be some mechanism maintaining the temperature in the optical part of the jet. Let us consider the possibility of heating the optical jet by Coulomb collisions of protons, since the jet is surrounded by interstellar matter which can play the role of the corona for the X-ray jet. The assumption that the ambient matter is isothermal is no longer valid, and we assume that the corona has a constant temperature, $T_0 = 2.2 \times 10^8$ K out to $r = r_{\rm cor} = 6.4 \times 10^{11}$ cm [1]; the matter is then cooled only by its expansion ($T \sim r^{-4/3}$). The matter density profile is

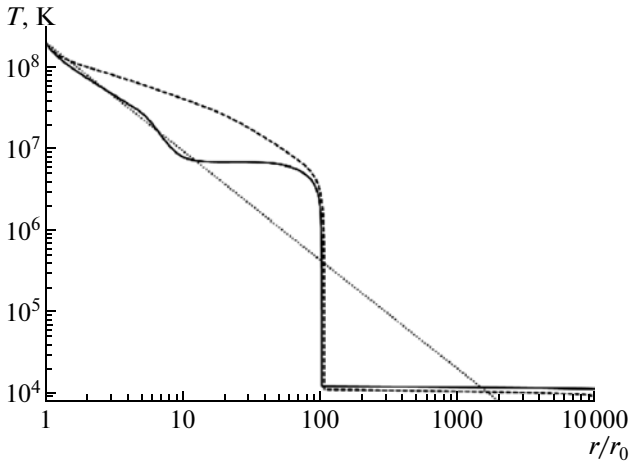

Fig. 7. Temperature profile of the jet taking into account radiative cooling and heating by Coulomb collisions for various functions $a(r)$. The dashed curve shows results for $a(r) \sim r^{-1.163}$ for $r < r_{\rm cor}$ and $a(r) \sim r^{-0.48}$ for $r > r_{\rm cor}$; the solid curve shows the case when the function $a(r)$ is chosen that the temperature profile is similar to the case of adiabatic expansion [see (62)]; the dotted curve shows the case of pure adiabatic cooling.

specified by (6) but with $n_{0,\rm cor} = 4.3 \times 10^{12}$ cm^{-3}. We have selected a form for the function $a(r)$ that enabled us to approximate the adiabatic curve at large distances fairly well (Fig. 7):

$$a(r) \qquad (62)$$
$$= \begin{cases} (r/r_0)^{-3/2}, & r < r_{\rm cor}, \\ 3.640 \times 10^{-2}(r/r_0)^{0.27}, & r_{\rm cor} < r < 11r_0, \\ 9.454 \times 10^{-2}(r/r_0)^{-0.128}, & \\ \quad 11r_0 < r < 100r_0, & \\ 5.243 \times 10^{3}(r/r_0)^{-2.5}, & r > 100r_0. \end{cases}$$

The functions are matched at the ends of the segments by the condition of continuity. Our calculations show that, with various choices for the function $a(r)$ in (61), it is possible to obtain an approximately constant temperature $T \approx 10^4$ K in the optical jet (Fig. 7).

6. CONCLUSION

We have shown that taking into account radiative cooling in the jet energy balance equation using data derived from modeling of the X-ray spectrum of SS 433 carried out in [1] leads to rapid jet cooling. The temperature falls off rapidly with radius, so that the implied length of the X-ray jet is much smaller than the observed length. This fact motivated us to investigate jet heating mechanisms in more detail.

A consideration of the contribution from Comptonization has shown that this mechanism can compensate for only a small part of the radiative losses.

We have considered a scenario with shocks travelling along the jet, heating the jet material when their energy is dissipated. The shocks are rapidly dissipated due to their radiation, and heat only narrow regions near the places of their origin. The entire jet could be heated, either due to the action of a wide spectrum of initial perturbations or interactions between the jet and ambient medium.

It seems that the most plausible mechanism is the conversion of the jet kinetic energy into thermal energy via Coulomb collisions between protons of the corona and jet. If a comparatively small magnetic field is present in the jet, $\sim$0.01 G, this heating can be efficient, and capable of compensating radiative losses. With a certain function characterizing heating due to Coulomb collisions, it is possible to obtain efficient heating of the entire X-ray jet. Heating due to interactions with protons of the stellar wind is able to maintain the observed temperature $\sim 10^4$ K in the optical jet. Since the kinetic energy flux in the jet greatly exceeds its radiative losses, the decrease in the jet velocity with radius is too small to be detected in existing observations.

ACKNOWLEDGMENTS

The work was partially supported by the Russian Foundatiaon for Basic Research (grant 11-02-00602), the State Program of Support for Leading Scientific Schools of the Russian Federation (grant NSh-3458.2010.1), and the Basic Research Program of the Presidium of the Russian Academy of Sciences "The Origin, Structure, and Evolution of Objects in the Universe." The work of Yu.M.K. was partially supported by a grant of the President of the Russian Federation for the State Support of Young Russian PhDs (MK-8696.2010.2) and the Fund for the Support of National Science.

REFERENCES

1. Yu. M. Krivosheyev, G. S. Bisnovatyi-Kogan, A. M. Cherepashchuk, and K. A. Postnov, Mon. Not. R. Astron. Soc. **394**, 1674 (2009).
2. G. S. Bisnovatyi-Kogan, *Physical Problems in the Theory of Stellar Evolution* (Nauka, Moscow, 1989) [in Russian].
3. E. V. Koval' and N. I. Shakura, in *Proceedings of the 23rd ESLAB Symposium on Two Topics in X-Ray Astronomy, Bologna, Italy, September 13–20, 1989,* Ed. by N. E. White, ESA SP-296 (Europ. Space Agency, 1989), Vol. 1, p. 479.
4. D. P. Cox and W. H. Tucker, Astrophys. J. **157**, 1157 (1969).

5. J. C. Raymond, D. P. Cox, and B. W. Smith, Astrophys. J. **204**, 290 (1976).
6. P. R. Shapiro and H. Kang, Astrophys. J. **318**, 32 (1987).
7. A. B. Kirienko, Astron. Lett. **19**, 11 (1993).
8. M. V. Barkov and G. S. Bisnovatyi-Kogan, Astron. Rep. **49**, 24 (2005).
9. *Physics of Space (The Small Encyclopedy)*, Ed. by R. A. Syunyaev (Sovetskaya Entsiklopediya, Moscow, 1986) [in Russian].
10. Ya. B. Zel'dovich and Yu. P. Raizer, *Physics of Shock Waves and High-Temperature Hydrodynamic Phenomena,* Vols. 1 and 2 (2nd ed., Nauka, Moscow, 1966; Academic Press, New York, 1966, 1967).
11. S. Fabrika, Astrophys. Space Phys. Rev. **12**, 1 (2004).
12. L. D. Landau and E. M. Lifshitz, *Course of Theoretical Physics,* Vol. 6: *Fluid Mechanics* (Nauka, Moscow, 1986; Pergamon, New York, 1987).
13. H. Marshall, C. Canizares, and N. Schulz, in *Chandra's First Decade of Discovery, Proceedings of the Conference, September 22–25, 2009, Boston, MA, USA,* Ed. by S. Wolk, A. Fruscione, and D. Swartz (2009), Abstract No. 149.
14. L. D. Landau and E. M. Lifshitz, *Course of Theoretical Physics,* Vol. 5: *Statistical Physics* (Nauka, Moscow, 1976; Pergamon, Oxford, 1980)
15. L. D. Landau and E. M. Lifshitz, *Course of Theoretical Physics,* Vol. 1: *Mechanics*, 4th ed. (Nauka, Moscow, 1988; Pergamon Press, New York, 1988).
16. L. D. Landau, Zh. Eksp. Teor. Fiz. **7**, 203 (1937).
17. K. Davidson and R. McCray, Astrophys. J. **241**, 1082 (1980).

Translated by K. Bronnikov